Strategies for braiding and ground state preparation in digital quantum hardware

Herasymenko, Y.

4 Bounds on nonlocal correlations in the presence of signaling and their application to topological zero modes

4.1 Introduction

In a Bell test [127, 128], Alice and Bob measure pairs of particles (possibly having a common source in their past) and then communicate in order to calculate the correlations between these measurements. The strength of empirical correlations enables one to characterize the underlying theory. In quantum mechanics, the above procedure corresponds to local measurements of Hermitian operators A_0/A_1 on Alice's side and B_0/B_1 on Bob's side. The correlators are defined using the quantum expectation value $c_{ij} = \langle A_i B_j \rangle$ and, when the operators have eigenvalues ± 1, it can be shown that the CHSH parameter obeys

$$|\mathcal{B}| \equiv |c_{00} + c_{10} + c_{01} - c_{11}| \leq 2\sqrt{2}, \tag{4.1.1}$$

which is known as the Tsirelson bound [129]. Stronger bounds on the correlators (i.e., bounds from which the Tsirelson bound can be derived) were proposed, e.g., by Uffink [130] and independently by Tsirelson, Landau and Masanes (TLM) [131–133]. The latter implies that

$$|c_{00}c_{10} - c_{01}c_{11}| \leq \sum_{j=0,1} \sqrt{(1 - c_{0j}^2)(1 - c_{1j}^2)}. \tag{4.1.2}$$

The TLM inequality is known to be necessary and sufficient for the correlators c_{ij} to be realizable in quantum mechanics [131–133] (implying, in particular, that if a set of correlators satisfies Eq. (4.1.2), it necessarily satisfies Eq. (4.1.1); the converse is not true). Importantly, when calculating

$\mathcal{B}$ in any local-realistic model it turns out that $|\mathcal{B}| \leq 2$, which is a famous variant of Bell's theorem known as the Clauser-Horne-Shimony-Holt (CHSH) inequality [134], which provides a measurable distinction between correlations achievable in local-realistic models and in quantum theory. These bounds, however, are not enough for fully characterizing the Alice-Bob quantum correlations. For the latter task, the Navascues-Pironio-Acin (NPA) hierarchical scheme of semidefinite programs was proposed [135].

All the above works plausibly assuming that Alice's and Bob's measurements are described by spatially local and Hermitian operators, implying that $[A_i, B_j] = 0$ for all i, j. As such, they cannot lead to superluminal signaling between Alice and Bob.

Trying, on the one hand, to generalize some of the above results, and on the other hand to pin-point the core reason they work so well, we relax below these two assumptions and examine the consequences of complex-valued correlations emerging from non-Hermitian non-commuting Alice and Bob operators. We thus allow a restricted form of signaling between the parties (similar to the one in [136]), but we maintain the Hilbert space structure, as well as other core ingredients of quantum mechanics. Surprisingly, the Tsirelson bound and TLM inequality remain valid in this generalized setting. Apart from that, we find intriguing relations between nonlocality, local correlations of Alice (or Bob), and signaling in the case of Hermitian yet non-commuting observables.

Considering non-Hermitian non-commuting observables may seem far from any sensible model. To alleviate this impression, we study an explicit example of a parafermionic system, which is a proper quantum system that provides a natural setting for comparing commuting and non-commuting sets of observables. The natural observables in the parafermionic system happen to be non-Hermitian. Parafermions (or rather parafermionic zero modes) are topological zero modes that generalize the better-known Majorana zero modes [6, 21, 113]. Parafermions can be realized in various quasi-one-dimensional systems [40, 137–142], see [143] for a comprehensive review. Similarly to the case of Majoranas, observables in a system of parafermions are inherently non-local as they comprise at least two parafermionic operators hosted at different spatial locations. In the case of Majoranas, this nonlocality is known to have manifestations through the standard CHSH inequality [144]. We do not follow the investigation line of Ref. [144], but rather investigate a different aspect of nonlocality, which is absent for Majoranas yet present for parafermions.

Specifically, we construct two examples. In the first, the system of parafermions is split into two spatially separated parts, A and B, with commuting observables $[A_i, B_j] = 0$. In the second example, Alice's and

Bob's parts are still spatially separated; the local permutation properties of A_0, A_1, as well as those of B_0, B_1 are exactly the same as in the first example, yet $[A_i, B_j] \neq 0$. This property alone has the potential to contradict relativistic causality since we have spatially separated observables which do not commute and thus allow for superluminal signaling (thus these systems can indeed simulate the case of non-Hermitian signaling operators). However, as we explain in Sec. 4.3.2, in order to measure their respective observables, Alice and Bob in our system must share a common region of space, which resolves the paradox. In this sense, Alice and Bob can be thought of as two experimenters acting on the same system. Therefore, the system of parafermions does not constitute a system in which the spatial and quantum mechanical notions of locality disagree. However, it simulates such a system (with spatial locality interpreted in a very naive way). Using these examples we investigate the theoretical bounds on correlations. We find that both systems obey the derived bounds. However, the maximal achievable correlations in the truly local system (first example) are significantly weaker than those of the non-local one.

Before we present our results in the next sections, one comment is due. One may think that investigating Bell-CHSH correlations with $[A_i, B_j] \neq 0$ is an abuse of notation. Originally introduced for distinguishing local-realistic theories from the standard quantum theory, the Bell-CHSH inequalities imply the use of conditional probabilities $P(a, b|i, j)$ that are defined in both. With $[A_i, B_j] \neq 0$, the correlators that have the same operator form are expressed not through probability distributions $P(a, b|i, j)$ but rather through quasiprobability distributions $W(a, b|i, j)$, cf. Appendix 4.C. Therefore, a formal replacement of commuting operators with non-commuting ones may seem an illegitimate operation in this context. We would like to emphasize that the key to comparing properties of different theories is considering objects that are defined in these theories in an operationally identical way. This is the reason that local-realistic theories are compared to quantum mechanics not in terms of the joint probability distribution $P(a_0, a_1, b_0, b_1)$ (that does not exist in quantum theory when $[A_i, A_j] \neq 0$ and/or $[B_i, B_j] \neq 0$) but in terms of $P(a, b|i, j)$ conditioned on the choice of observables: $P(a, b|i, j)$ are defined in both theories and can be measured by the same measurement procedure. Since our aim here is to compare the standard quantum theory with that allowing for $[A_i, B_j] \neq 0$, working in the language of correlators that are defined and can be measured (even if they are complex) by means of weak measurements in both theories [145] is a natural decision. We thus compare nonlocal theories having a Hilbert space structure, rather

than a probabilistic structure (common, e.g., to local hidden variables theories and quantum mechanics, but not to the post-quantum theories discussed here). However, in the case of the standard quantum theory, the correlation functions (and thus our new bounds) can be expressed in terms of $P(a,b|i,j)$, making them new bounds on the possible probability distributions in the standard quantum theory.

In what follows, we start in Sec. 4.2 by defining an operator-based (rather than probability-based) notion of complex correlations arising in nonlocal, non-Hermitian systems admitting signaling and then find the generalized inequalities bounding them. Importantly, this notion has an operational sense in terms of weak measurements, as discussed in the Appendix 4.C.2. In Sec. 4.3, we review parafermionic systems and show they can simulate such non-Hermitian signaing systems. We then numerically prove they are indeed bounded by the proposed bounds. Sec. 4.4 concludes the chapter. Some technical details appear in the Appendices.

4.2 Analytic results for correlations of general non-Hermitian non-commuting operators

Below we prove a number of bounds on quantum correlations of non-Hermitian non-commuting operators. We generalize the Tsirelson and the TLM bounds (Theorems 1 and 2, which have been previously derived for Hermitian commuting operators, see [146]) and derive previously unknown bounds (Theorems 3 and 4, which are applicable to the Hermitian, non-signaling case as well). Here we introduce the bounds and discuss them, while their proofs are deferred to Sec. 4.2.1. The bounds are expressed in terms of Pearson correlation functions of operators X and Y defined as

$$C(X,Y)=\frac{\langle XY^{\dagger}\rangle-\langle X\rangle\langle Y\rangle^{\dagger}}{\Delta_X\Delta_Y}, \tag{4.2.1}$$

where $\Delta_X=\sqrt{\langle XX^{\dagger}\rangle-|\langle X\rangle|^2}$ is the variance of X (which is assumed to be non-zero), and averaging is performed with respect to some state $|\psi\rangle$ in the Hilbert space. This definition is a straightforward generalization of the usual Pearson correlation between commuting Hermitian operators. The Pearson correlations reduce to the standard $c_{XY}=\langle XY\rangle$ for Hermitian X and Y on states $|\psi\rangle$ such that $\langle X\rangle=\langle Y\rangle=0$ and $\Delta_X=\Delta_Y=1$. We note that $C(X,Y)$ is ill-defined when $\Delta_X=0$ or $\Delta_Y=0$; yet, as we show

in Sec. 4.2.1, $|C(X,Y)| \leq 1$ everywhere, including the vicinity of such special points.

For the case of commuting operators X, Y, the definition of $C(X,Y)$ can be expressed in terms of the joint probability distributions, and our below bounds can be thought of as restricting the possible probability distributions in quantum theory. When X and Y do not commute, this is not the case, which defies the notions that conventionally underlie Bell inequalities. However, our aim here is not to analyze complex local hidden variables models but rather to examine general models which are manifestly nonlocal. In particular, we wish to analyze whether known bounds on quantum correlations remain effective when generalized to cases of non-Hermitian signaling operators. We argue that these complex correlations are physically meaningful because there is an empirical protocol for measuring them. That operational meaning of the above correlations in terms of weak measurements is given in Appendix 4.C.2. Alternatively, for the case of non-commuting observables, $C(X,Y)$ can be expressed in terms of quasiprobability distibutions, and thus our bounds restrict possible quasiprobability distributions in that case. We discuss this in detail in Appendix 4.A.

We now discuss the bounds on Alice-Bob correlations.

Theorem 1. ***(Generalized Tsirelson bound).*** *Define* $\mathcal{B} \stackrel{\text{def}}{=} C(A_0,B_0) + C(A_1,B_0) + C(A_0,B_1) - C(A_1,B_1)$ *as the complex-valued Bell-CHSH parameter of any operators* A_i *and* B_j*. The following holds*

$$\begin{aligned} |\mathcal{B}| &= \sqrt{\mathrm{Re}(\mathcal{B})^2 + \mathrm{Im}(\mathcal{B})^2} \\ &\leq \sqrt{2}\left[\sqrt{1+\mathrm{Re}(\eta)} + \sqrt{1-\mathrm{Re}(\eta)}\right] \\ &\leq 2\sqrt{2}, \end{aligned} \tag{4.2.2}$$

where η *is either* $C(A_0,A_1)$ *or* $C(B_0,B_1)$ *(the one having the larger* $|\mathrm{Re}(\eta)|$ *among them will give rise to a tighter inequality).*

Despite the fact that $C(X,Y) \neq c_{XY}$, the Bell-CHSH parameter defined through $C(X,Y)$ obeys the same Tsirelson bound as for c_{XY} in Eq. (4.1.1). Moreover, the proof of the Tsirelson bound for $C(X,Y)$ is valid independently of whether $[A_i,B_j]=0$. A somewhat tighter bound (the middle row of Eq. (4.2.2)) is obtained in terms of η that expresses on-site correlations on Alice's or Bob's side. This is also insensitive to whether $[A_i,B_j]=0$.

Theorem 2. ***(Generalized TLM bound).*** *The following holds for any*

operators A_i, B_j, $i,j \in \{0,1\}$,

$$\left|C(B_0,A_0)^\dagger C(B_0,A_1) - C(B_1,A_0)^\dagger C(B_1,A_1)\right| \leq \sum_{j=0,1} \sqrt{(1-|C(B_j,A_0)|^2)(1-|C(B_j,A_1)|^2)}. \quad (4.2.3)$$

Similarly to the previous theorem, this bound is insensitive to whether $[A_i,B_j]=0$ and has the same form as the standard TLM bound, Eq. (4.1.2), modulo replacing $C(X,Y)$ with real-valued c_{XY}.

We note in passing that our bounds apply to both operators with bounded and unbounded spectrum. Implementing Bell tests in mesoscopic systems often requires dealing with operators having an unbounded spectrum, cf. Ref. [147]. Our theorems 1 and 2 may thus be useful for studies in such systems.

Theorem 3. ***(Relation between nonlocality, local correlations, and signaling)***. *Let $\mathcal{B}$ be the complex-valued Bell-CHSH parameter defined in Theorem 1. Then,*

$$\left(\frac{\mathrm{Re}(\eta)}{2}\right)^2 + \left(\frac{\mathrm{Re}(\mathcal{B})}{2\sqrt{2}}\right)^2 + \left(\frac{\mathrm{Im}(\mathcal{B})}{2\sqrt{2}}\right)^2 \leq 1. \quad (4.2.4)$$

This bound is also valid independently of $[A_i,B_j]=0$. In the case of Hermitian A_i, B_j that obey $[A_i,B_j]=0$, $C(A_i,B_j)$ is real, implying $\mathrm{Im}(\mathcal{B})=0$. If A_i and B_j are Hermitian but do not mutually commute, there can appear imaginary components to $C(A_i,B_j)$ and $\mathcal{B}$. Therefore, this relation may be interpreted as a constraint on non-local correlations (represented by $\mathrm{Re}(\mathcal{B})/(2\sqrt{2})$), local on-site correlations ($\mathrm{Re}(\eta)/2$), and signaling (represented by $\mathrm{Im}(\mathcal{B})/(2\sqrt{2}) \neq 0$). These three quantities are thus confined to the unit ball.

Theorem 4. *Let $\mathcal{B}$ be the complex-valued Bell-CHSH parameter defined in Theorem 1. In the case of isotropic correlations, $C(A_i,B_j)=(-1)^{ij}\varrho$ (such that $\mathcal{B}=4\varrho$) for some complex-valued ϱ,*

$$|\eta|^2 + \left(\frac{\mathrm{Re}(\mathcal{B})}{2\sqrt{2}}\right)^2 + \left(\frac{\mathrm{Im}(\mathcal{B})}{2\sqrt{2}}\right)^2 \leq 1. \quad (4.2.5)$$

Note that Eq. (4.2.5) provides a tighter bound than Eq. (4.2.4). However, Eq. (4.2.5) is proved under the rather restrictive assumption of $C(A_i,B_j) =$

$(-1)^{ij}\varrho$. This is a valid assumption within non-signaling theories in the following sense. Reference [148] argued that the standard Bell-CHSH parameter $\mathcal{B} = c_{00} + c_{10} + c_{01} - c_{11}$ for ± 1-valued observables in a non-signaling theory (not necessarily classical or quantum) can always be maximized on a state satisfying $c_{ij} = (-1)^{ij}\rho$ with a real ρ. While the statement of Ref. [148] was proved for the standard correlations c_{XY} (and not our $C(X,Y)$) and maximizing the l.h.s. of Eq. (4.2.5) is not equivalent to maximizing $|\mathcal{B}|$, one might hope that the possibility of arranging $C(A_i, B_j) = (-1)^{ij}\varrho$ is related to non-signaling, and the bound of Eq. (4.2.5) would discriminate the cases of $[A_i, B_j] = 0$ and $[A_i, B_j] \neq 0$. We provide some numerical evidence for the last statement in Sec. 4.3.

4.2.1 Proofs of analytic bounds

Lemma 1. ***(Generalized uncertainty relations, see Ref. [149] for elaboration on the term).*** *Denote by $X_1, \ldots, X_n$, a number of operators. Let C be an $n \times n$ Hermitian matrix whose ij-th entry is*

$$C(X_i, X_j) = \frac{\langle X_i X_j^\dagger \rangle - \langle X_i \rangle \langle X_j \rangle^\dagger}{\Delta_{X_i} \Delta_{X_j}}, \tag{4.2.6}$$

where $\Delta_X = \sqrt{\langle XX^\dagger \rangle - |\langle X \rangle|^2}$ is the uncertainty in X (which is assumed to be non-zero). Then $C \succeq 0$, i.e., it is positive semidefinite.

Proof. Denote $|\psi\rangle$, the underlying quantum state. For any n-dimensional vector, $v^T = [v_1, \ldots, v_n]$, it follows that

$$v^T D C D^T v = \langle \phi | \phi \rangle \geq 0, \tag{4.2.7}$$

where D is a (positive semidefinite) diagonal matrix whose entries are $D_{ii} = \Delta_{X_i}$, and $|\phi\rangle = \sum_{i=1}^n v_i \left(X_i - \langle X_i \rangle\right) |\psi\rangle$. Therefore, $DCD^T \succeq 0$ and so is $C \succeq 0$. □

Applying this lemma to two operators, X_1, X_2, one obtains an inequality $|C(X_1, X_2)| \leq 1$, implying that the correlation functions are bounded even near $\Delta_{X_{1,2}} = 0$.

Theorem 1. *Proof.* Construct the matrix C for the operators A_0, A_1,

and B_j,

$$\begin{bmatrix} C(B_j,B_j) & C(B_j,A_1) & C(B_j,A_0) \\ C(B_j,A_1)^\dagger & C(A_1,A_1) & C(A_0,A_1) \\ C(B_j,A_0)^\dagger & C(A_0,A_1)^\dagger & C(A_0,A_0) \end{bmatrix} = \begin{bmatrix} 1 & C(B_j,A_1) & C(B_j,A_0) \\ C(B_j,A_1)^\dagger & 1 & \eta \\ C(B_j,A_0)^\dagger & \eta^\dagger & 1 \end{bmatrix} \succeq 0, \quad (4.2.8)$$

where $\eta \stackrel{\text{def}}{=} C(A_0,A_1)$. By the Schur complement condition for positive semidefiniteness this is equivalent to

$$C^A \stackrel{\text{def}}{=} \begin{bmatrix} 1 & \eta \\ \eta^\dagger & 1 \end{bmatrix} \succeq \begin{bmatrix} C(B_j,A_1)^\dagger \\ C(B_j,A_0)^\dagger \end{bmatrix} \begin{bmatrix} C(B_j,A_1) & C(B_j,A_0) \end{bmatrix}. \quad (4.2.9)$$

Let $v_j^T = [(-1)^j, 1]$. The above inequality implies

$$\begin{aligned} 2(1+(-1)^j \mathrm{Re}(\eta)) &= v_j^T C^A v_j \\ &\geq \left| C(B_j,A_0) + (-1)^j C(B_j,A_1) \right|^2. \end{aligned} \quad (4.2.10)$$

This together with the triangle inequality yield

$$\begin{aligned} |\mathcal{B}| &\leq \sum_{j=0,1} \left| C(B_j,A_0) + (-1)^j C(B_j,A_1) \right| \\ &\leq \sqrt{2} \sum_{j=0,1} \sqrt{1+(-1)^j \mathrm{Re}(\eta)}, \end{aligned} \quad (4.2.11)$$

which completes the proof. Note that by swapping the roles of A and B, a similar inequality is obtained where $\eta = C(B_0,B_1)$. □

Theorem 2. *Proof.* The inequality (4.2.9) implies

$$\begin{aligned} &(1-|C(B_j,A_0)|^2)(1-|C(B_j,A_1)|^2) \\ &\qquad - \left| \eta - C(B_j,A_0)^\dagger C(B_j,A_1) \right|^2 \geq 0, \end{aligned} \quad (4.2.12)$$

which follows from the non-negativity of the determinant of the matrix obtained by subtracting the right hand side from the left hand side in (4.2.9). Therefore,

$$\begin{aligned} &\left| \eta - C(B_j,A_0)^\dagger C(B_j,A_1) \right| \\ &\qquad \leq \sqrt{(1-|C(B_j,A_0)|^2)(1-|C(B_j,A_1)|^2)}. \end{aligned} \quad (4.2.13)$$

This and the triangle inequality give rise to the theorem,

$$\begin{aligned}\left|C(B_0,A_0)^\dagger C(B_0,A_1)-C(B_1,A_0)^\dagger C(B_1,A_1)\right| &\\ \leq \sum_{j=0,1}\left|\eta - C(B_j,A_0)^\dagger C(B_j,A_1)\right| &\\ \leq \sum_{j=0,1}\sqrt{(1-|C(B_j,A_0)|^2)(1-|C(B_j,A_1)|^2)}. \quad \square \quad (4.2.14)\end{aligned}$$

Theorem 3. *Proof.* We have seen that

$$|\mathcal{B}| \leq \sqrt{2}\left(\sqrt{1+\mathrm{Re}(\eta)}+\sqrt{1-\mathrm{Re}(\eta)}\right). \quad (4.2.15)$$

Therefore,

$$|\mathcal{B}|^2 = \mathrm{Re}(\mathcal{B})^2+\mathrm{Im}(\mathcal{B})^2 \leq 4\left(1+\sqrt{1-\mathrm{Re}(\eta)^2}\right). \quad (4.2.16)$$

Because, $\sqrt{1-a} \leq 1-a/2$ for $a \in [0,1]$, it follows that

$$\mathrm{Re}(\mathcal{B})^2+\mathrm{Im}(\mathcal{B})^2 \leq 8-2\mathrm{Re}(\eta)^2, \quad (4.2.17)$$

from which the theorem follows. □

Theorem 4. *Proof.* In case the isotropy holds, i.e., $C(A_i,B_j) = C(B_j,A_i)^* = (-1)^{ij}\varrho$, (4.2.12) reads

$$\left|\eta-(-1)^j|\varrho|^2\right|^2 \leq (1-|\varrho|^2)^2, \quad (4.2.18)$$

and thus

$$|\eta|^2-2(-1)^j|\varrho|^2\mathrm{Re}(\eta) \leq 1-2|\varrho|^2. \quad (4.2.19)$$

Averaging both sides in this inequality over $j=0,1$, and rearranging give

$$|\eta|^2+2|\varrho|^2 \leq 1. \quad (4.2.20)$$

Finally, substituting $\varrho = \mathcal{B}/4$ into (4.2.20) yields the theorem. □

4.3 Investigating the bounds in the system of parafermions

Parafermions provide a unique test system for the bounds proven in the previous section. First, the natural observables in a system of parafermions

are non-Hermitian. Second, in this system the non-commutativity between Alice's and Bob's operators can be switched on and off without changing anything else about the algebra of operators, enabling a clean investigation of the effect of Alice-Bob non-commutativity. Finally, there have been a number of proposals for experimental implementations of parafermions [40, 137–142], which opens the way for experimental verification of our predictions.

The structure of the section is as follows. In Sec. 4.3.1, we give a brief introduction to the physics of parafermions and the algebra of their operators. In Sec. 4.3.2, we construct the observables of Alice and Bob. Those not interested in the physics of parafermions may skip directly to Eqs. (4.3.8–4.3.10) detailing the permutation relations of the observables and Eqs. (4.3.11–4.3.16) introducing their explicit matrix representation. In Sec. 4.3.3, we provide the results of the numerical investigation of bounds (4.2.2–4.2.5).

4.3.1 Parafermion physics and algebra

Parafermionic zero modes can be created in a variety of settings [40, 137–142]. In different settings, they have subtly different properties. We focus on parafermions implemented with the help of fractional quantum Hall (FQH) edges proximitized by a superconductor [40, 137, 140]. The setup employs two FQH puddles of the same filling factor ν (grey regions in Fig. 4.1a) separated by vacuum. This gives rise to two counter-propagating chiral FQH edges. The edges can be gapped either by electron tunneling between them (T domains) or by proximity-induced superconducting pairing of electrons at the edges (SC domains). Domain walls between the domains of two types host parafermionic zero modes $\alpha_{s,j}$ with $s = R/L = \pm 1$ denoting whether a parafermion belongs to the right- or left-propagating edge respectively, and j denoting the domain wall number.

Parafermion operators have the following properties:

$$\alpha_{s,j}^{2/\nu} = \alpha_{s,j}\alpha_{s,j}^\dagger = \alpha_{s,j}^\dagger\alpha_{s,j} = 1, \tag{4.3.1}$$

$$\alpha_{s,j}\alpha_{s,k} = \alpha_{s,k}\alpha_{s,j}e^{i\pi\nu s\mathrm{sgn}(k-j)}, \tag{4.3.2}$$

$$\alpha_{R,j}\alpha_{L,k} = \alpha_{L,k}\alpha_{R,j}\begin{cases} e^{i\pi\nu} & , k \neq j, \\ 1 & , k = j \text{ are even}, \\ e^{2i\pi\nu} & , k = j \text{ are odd}, \end{cases} \tag{4.3.3}$$

where sgn is the sign function. These properties are valid for $\nu = 1/(2m+1)$, $m \in \mathbb{Z}_+$ considered in Refs. [40, 137] and for $\nu = 2/3$ considered in

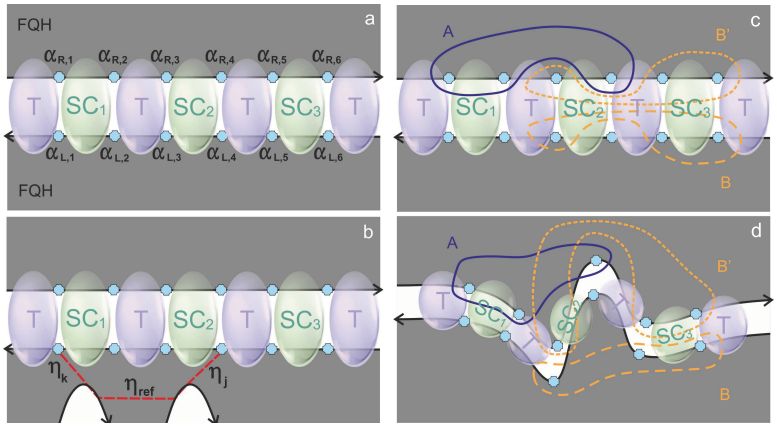

Figure 4.1: a, b — A physical setup for creating and measuring parafermions. a — Setup for implementing parafermions (represented in cyan) with two fractional quantum Hall (FQH) edges (arrows) supporting a series of electron-tunneling-gapped (T) and superconductivity-gapped (SC) domains. b — Setup for measuring parafermionic observables with the help of two additional FQH edges (curved arrows) as in Ref. [150] (cf. Appendix 4.B). c, d — Parafermionic observables and their mutual locality. c — Grouping parafermions into groups belonging to Alice (A) and Bob (B/B'). d — A and B do not have common parafermions, are mutually local, and can be made arbitrarily distant in space. While A and B' do not have common parafermions, they are not mutually local: for Alice to measure A while Bob can measure B', there should be a region of the upper FQH puddle accessible both to Alice and Bob.

Ref. [140]. In the case of $\nu = 1$, parafermions reduce to Majorana operators and $\alpha_{R,j} = \alpha_{L,j}$.

The physics of parafermions is associated with degenerate ground states of the system. Namely, beyond hosting Cooper pairs, each superconducting domain SC_j can host a certain charge Q_j (mod$2e$) quantized in the units of charge of FQH quasiparticles νe. Thus each Q_j has $d = 2/\nu$ distinct values, and the ground state degeneracy of a system as in Fig. 4.1a is therefore $d^{N_{\mathrm{SC}}}$, where N_{SC} is the number of SC domains. Parafermionic operators $\alpha_{s,j}$ act in this degenerate space of ground states and represent the effect of adding a FQH quasiparticle to the system from a FQH puddle corresponding to s at domain wall j. Various observables in the system of parafemions can be expressed through unitary operators $\alpha_{s,j}\alpha^\dagger_{s,k}$. In particular, Q_j themselves can be expressed through $e^{i\pi s(Q_j/e-\nu/2)} = (-1)^{2/\nu}\alpha^\dagger_{s,2j-1}\alpha_{s,2j}$. One can show that $\left(\alpha_{s,j}\alpha^\dagger_{s,k}\right)^d = -e^{2i\pi/\nu}$, which implies that $\alpha_{s,j}\alpha^\dagger_{s,k}$ has d distinct eigenvalues, all having the form $-e^{i\pi\nu(r+1/2)}$ with $r \in \mathbb{Z}$.

Unitary operators $\alpha_{s,j}\alpha^\dagger_{s,k}$ are thus natural "observables" in the system despite being non-Hermitian. The permutation relations of such operators immediately follow from Eqs. (4.3.1-4.3.3). Despite being spatially disconnected, such operators composed of different pairs of parafermions may not commute, e.g.,

$$\alpha_{R,2}\alpha^\dagger_{R,4}\alpha_{R,3}\alpha^\dagger_{R,5} = \alpha_{R,3}\alpha^\dagger_{R,5}\alpha_{R,2}\alpha^\dagger_{R,4}e^{2i\pi\nu}. \tag{4.3.4}$$

It is interesting to note that in the case of Majoranas ($\nu = 1$), none of these two unique properties would hold: the operators $i\alpha_{s,j}\alpha^\dagger_{s,k}$ would be Hermitian, while two such operators having no common Majoranas would commute.

4.3.2 Alice's and Bob's observables

For a parfermionic system with three SC domains (as in Fig. 4.1) with a fixed total charge, the ground state is d^2-degenerate, which allows to split it into two distinct subsystems: SC_1 and SC_3 domains, each having degeneracy d as each can have d distinct values of charge Q_j. The charge of SC_2 domain is determined by the state of SC_1 and SC_3 in order for the total charge to be fixed. This system is thus a natural candidate for studying quantum correlations between two subsystems. To this end, we introduce observables accessible to Alice,

$$A_0 = \alpha_{R,2}\alpha^\dagger_{R,4}, \quad A_1 = \alpha_{R,1}\alpha^\dagger_{R,4}, \tag{4.3.5}$$

and two different sets of observables accessible to Bob:

$$B_0 = \alpha_{L,3}\alpha_{L,5}^{\dagger}, \quad B_1 = \alpha_{L,3}\alpha_{L,6}^{\dagger}, \tag{4.3.6}$$

and

$$B_0' = \alpha_{R,3}\alpha_{R,6}^{\dagger}, \quad B_1' = \alpha_{R,3}\alpha_{R,5}^{\dagger}. \tag{4.3.7}$$

They have identical local algebra, yet different commutation properties of Alice's and Bob's observables:

$$A_0 A_1 = A_1 A_0 e^{-i\pi\nu}, \tag{4.3.8}$$

$$B_0 B_1 = B_1 B_0 e^{-i\pi\nu}, \quad B_0' B_1' = B_1' B_0' e^{-i\pi\nu}, \tag{4.3.9}$$

$$[A_j, B_k] = 0, \quad A_j B_k' = B_k' A_j e^{2i\pi\nu}. \tag{4.3.10}$$

The non-commutation of A and B' observables would imply the possiblity of superluminal signaling had the observables been truly spatially separate (which is not the case, as we explain below). Therefore, we call the set of A and B a non-signaling set, and the set of A and B' a signaling set of observables.

Naively, Alice's observables are local with respect to either set of Bob's observables, cf. Fig. 4.1c. Indeed, A and either the B or B' set use different parafermions, which can be made arbitrarily distant from each other, cf. Fig. 4.1d. However, the locality issue in this system is subtler as in order to probe an observable of the form $\alpha_{s,j}\alpha_{s,k}^{\dagger}$, one needs to enable FQH quasiparticle tunneling to both parafermions simultaneously (see Appendix 4.B). At the same time, quasiparticles can tunnel to a parafermion only from the FQH puddle corresponding to the parafermion index s, not through vacuum and not from the other puddle. Therefore, as can be seen from Fig. 4.1d, the A and B sets are indeed mutually local, while A and B' are not. The ability of Alice to measure observables in A and of Bob to measure observables in B', requires them to have access to a common region of the upper FQH puddle. Thus, the system does not violate the laws of quantum mechanics, nor exhibits superluminal signaling. Nevertheless, it presents a unique opportunity for comparing correlations of commuting and non-commuting (but otherwise equivalent) sets of observables.

The standard tool for studying quantum correlations is given by Bell inequalities. However, since the observables considered here have more than two eigenvalues, we require CHSH-like inequalities suitable for multi-outcome measurements. We study the inequalities introduced in Theorems 1–4, as well as an inequality from Ref. [151]. These inequalities

involve correlators of the form $\langle A_j B_k^\dagger \rangle$ and $\langle A_j \, (B_k')^\dagger \rangle$. Since $[A_j, B_k] = 0$, $\langle A_j B_k^\dagger \rangle$ can be experimentally obtained by performing strong measurements of A_j and B_k separately according to the protocol of Appendix 4.B and then calculating the correlations. Alternatively, these correlations can be measured with weak measurements [67, 68]. The non-commutativity of A_j and B_k' does not allow for a strong-measurement-based approach in the case of $\langle A_j \, (B_k')^\dagger \rangle$. However, this correlator can be measured with the help of weak measurements as described in Appendix 4.C.

From now on we focus on parafermions implemented using $\nu = 2/3$ FQH puddles. Using permutation relations (4.3.8–4.3.10) supplemented by the permutation relations of B_j and B_k', as well as $\left(\alpha_{s,j}\alpha_{s,k}^\dagger\right)^3 = 1$, one can derive an explicit matrix representation for observables (4.3.5–4.3.7):

$$A_0 = \begin{pmatrix} 1 & 0 & 0 \\ 0 & e^{2\pi i/3} & 0 \\ 0 & 0 & e^{-2\pi i/3} \end{pmatrix} \otimes \begin{pmatrix} 1 & 0 & 0 \\ 0 & 1 & 0 \\ 0 & 0 & 1 \end{pmatrix}, \tag{4.3.11}$$

$$A_1 = \begin{pmatrix} 0 & 1 & 0 \\ 0 & 0 & 1 \\ 1 & 0 & 0 \end{pmatrix} \otimes \begin{pmatrix} 1 & 0 & 0 \\ 0 & 1 & 0 \\ 0 & 0 & 1 \end{pmatrix}, \tag{4.3.12}$$

$$B_0 = \begin{pmatrix} 1 & 0 & 0 \\ 0 & 1 & 0 \\ 0 & 0 & 1 \end{pmatrix} \otimes \begin{pmatrix} 1 & 0 & 0 \\ 0 & e^{2\pi i/3} & 0 \\ 0 & 0 & e^{-2\pi i/3} \end{pmatrix}, \tag{4.3.13}$$

$$B_1 = \begin{pmatrix} 1 & 0 & 0 \\ 0 & 1 & 0 \\ 0 & 0 & 1 \end{pmatrix} \otimes \begin{pmatrix} 0 & 1 & 0 \\ 0 & 0 & 1 \\ 1 & 0 & 0 \end{pmatrix}, \tag{4.3.14}$$

$$B_0' = \begin{pmatrix} 0 & e^{-2\pi i/3} & 0 \\ 0 & 0 & e^{2\pi i/3} \\ 1 & 0 & 0 \end{pmatrix} \otimes \begin{pmatrix} 0 & 1 & 0 \\ 0 & 0 & 1 \\ 1 & 0 & 0 \end{pmatrix}, \tag{4.3.15}$$

$$B_1' = \begin{pmatrix} 0 & e^{-2\pi i/3} & 0 \\ 0 & 0 & e^{2\pi i/3} \\ 1 & 0 & 0 \end{pmatrix} \otimes \begin{pmatrix} 0 & 0 & 1 \\ e^{-2\pi i/3} & 0 & 0 \\ 0 & e^{2\pi i/3} & 0 \end{pmatrix}. \tag{4.3.16}$$

This is used in the numerical investigation in the next section.

Bound:		I_3	Tsirelson type	TLM-type, l.h.s/r.h.s.	L.h.s. of (4.2.4)	L.h.s. of (4.2.5)
Theoretical maximum		2.91 [152]	$2\sqrt{2}$ (≈ 2.83)	1	1	1 (if assumptions hold)
Parafermion maximum	non-signaling (A+B)	2.60	2.44	0.71	0.74	1.00
	signaling (A+B')	2.60	2.82	1.00	1.00	1.56

Table 4.1: Characterization of various bounds on non-local correlations for the signaling and non-signaling sets of parafermionic observables. Maximal values achieved with parafermionic observables ('Parafermion maximum') are compared to the theoretical maximum. The quantities considered are I_3 (4.3.17, l.h.s.), generalized Tsirelson (4.2.2, l.h.s.), generalized TLM (4.2.3, l.h.s/r.h.s.), relation (4.2.4, l.h.s.), and relation (4.2.5, l.h.s.).

4.3.3 Numerical results for correlations of parafermions

Here we numerically investigate the bounds on correlations presented above (4.2.2–4.2.5) and the CHSH-like inequality derived in Ref. [151]. The inequality of Ref. [151] states that for a local-realistic system

$$I_3 = Q_{00} + Q_{01} - Q_{10} + Q_{11} \leq 2, \tag{4.3.17}$$

where $Q_{jk} = \mathrm{Re}\left[\langle A_j B_k \rangle\right] + \frac{1}{\sqrt{3}} \mathrm{Im}\left[\langle A_j B_k \rangle\right]$ for $i \geq j$, and $Q_{01} = \mathrm{Re}\left[\langle A_0 B_1 \rangle\right] - \frac{1}{\sqrt{3}} \mathrm{Im}\left[\langle A_0 B_1 \rangle\right]$. The observables are assumed to have possible values (for the quantum case that we are interested in, eigenvalues) $e^{2\pi i r/3}$, $r \in \mathbb{Z}$, which is the case for the observables defined in Eqs. (4.3.11–4.3.16). In the standard quantum theory, i.e., for quantum observables such that $[A_j, B_k] = 0$, the maximum attainable value is known to be ≈ 2.91 [152].

For all the inequalities investigated, we calculated the corresponding correlations $C(A_i, B_j)$ or $\langle A_j B_k \rangle$, and maximized the relevant expressions numerically over all possible states $|\psi\rangle$. The expressions maximized were the left-hand side of bounds (4.3.17, 4.2.2, 4.2.4, 4.2.5) and the ratio of the left-hand side to the right-hand side of inequality (4.2.3). The numerical maximization was performed independently via Wolfram Mathematica (functions `NMaximize` for finding the global maximum and `FindMaximum` for investigating local maxima) and Python (package `scipy.optimize`, functions `basinhopping` for finding the global maximum with `SLSQP` optimization method for investigating local maxima). One aspect deserves

mentioning. Correlation functions $C(A_i, B_j)$ defined in Eq. (4.2.6) are not well-defined in all of the Hilbert space as the denominator can turn out to be zero. However, the points where it does, constitute a set of measure zero among all the states. Moreover, in the vicinity of these special points, $C(A_i, B_j)$ does not diverge but stays bounded as $|C(A_i, B_j)| \leq 1$; however, the limiting value as one approaches the special point depends on the direction of approach. Therefore, with careful treatment, these special points do not constitute a problem for investigation. Namely, we replaced $\Delta_{A_i} \to \Delta_{A_i} + \epsilon^2$, $\Delta_{B_j} \to \Delta_{B_j} + \epsilon^2$ with a small cutoff ϵ, and checked that our results do not change as $\epsilon \to 0$. Furthermore, the states $|\psi\rangle$ on which the maximum values in Table 4.1 are achieved are such that $\Delta_{A_i}, \Delta_{B_j} \neq 0$ for all A_i, B_j.

The results of our investigation are presented in Table 4.1. First, we note that the l.h.s. of Eq. (4.3.17) does not distinguish the signaling and non-signaling sets of observables. Second, our bounds (4.2.2-4.2.4) are obeyed by both sets. However, the signaling set saturates the bounds much better than the non-signaling one. Finally, the bound of Theorem 4, (4.2.5), is saturated by the non-signaling set and *violated* by the signaling one. This does not contradict the proof, which assumes $C(A_i, B_j) = (-1)^{ij}\varrho$. In fact, this property is not satisfied by the states $|\psi\rangle$ maximizing the l.h.s. of (4.2.5) for either of the sets. However, this numerical evidence together with the fact that $C(A_i, B_j) = (-1)^{ij}\varrho$ correlations might be special for non-signaling theories (cf. the discussion after Theorem 4) imply that Eq. (4.2.5) may be a good bound for distinguishing signaling and non-signaling quantum theories. We provide further evidence for the last statement in Appendix 4.D.

4.4 Discussion

Our analytic results have important implications for understanding quantum correlations. It is known that the standard CHSH parameter has distinct bounds for classical local ($|\mathcal{B}| \leq 2$) and non-local ($|\mathcal{B}| \leq 4$) hidden variable theories, while the standard quantum theory obeys the Tsirelson bound (4.1.1). Our variation of the Tsirelson bound (4.2.2) is closely related to the original Tsirelson bound. In particular, for Hermitian observables $X = A_i, B_j$ such that $XX^\dagger = 1$ and states $|\psi\rangle$ such that $\langle\psi|X|\psi\rangle = 0$, our Bell-CHSH parameter $|\mathcal{B}|$ (4.2.2) coincides with the original one. At the same time, our proof shows that the Tsirelson bound (4.2.2), as well as the TLM bound (4.2.3), do not distinguish between the standard and non-local signaling quantum theories. This implies that the Hilbert space

structure is much more restrictive than it was previously thought (see, e.g., Eq. 4.2.8 which underlies our proofs). Naively, one could expect that the possibility of signaling would allow nonlocal correlations to be stronger than quantum, because one party can directly affect from a distance the others' outcomes and in particular make them more correlated with hers. However, the limited kind of signaling we have introduced here, still within a quantum-like structure, is insufficient for this purpose.

At the same time, understanding the bounds on correlations in the standard quantum theory, that explicitly takes into account the absence of signaling, may be beneficial both for deepening its understanding, further testing its validity, and deriving bounds on protocols for quantum information processing. Our numerical results with parafermions provide a candidate for such a bound, Eq. (4.2.5). Indeed, the "non-signaling" parafermionic set stayed within the bound, while the "signaling" one violated it. Moreover, Ref. [148] argued that the assumptions we used to prove theorem 4 hold generally for the states maximizing the standard Bell-CHSH parameter in non-signaling theories (not in the sense that any maximizing state satisfies the assumptions, but in the sense that it is always possible to find a state that maximizes the standard Bell-CHSH parameter and satisfies the assumptions). Therefore, we believe that inequality (4.2.5) deserves further investigation.

4.A Relation between the correlation functions $C(X,Y)$ and joint probability distributions

For the standard case of commuting operators X and Y, it is possible to express correlators $C(X,Y)$ defined in Eq. (4.2.1) through the joint probability distribution $P(x,y)$ of outcomes of X and Y measurements. Indeed, for commuting X and Y, it is possible to find their common eigenbasis $|xy\lambda\rangle$, where $X|xy\lambda\rangle = x|xy\lambda\rangle$ and similarly for Y; λ represents possible additional quantum numbers. Then any state allows for a decomposition

$$|\psi\rangle = \sum_{x,y,\lambda} \alpha_{xy\lambda}|xy\lambda\rangle. \tag{4.A.1}$$

The probability of one observer obtaining x in a measurement of X, while the other obtains y in a measurement of Y is given by

$$P(x,y) = \mathrm{Tr}|\psi\rangle\langle\psi|\mathcal{P}_x^{(X)}\mathcal{P}_y^{(Y)} = \sum_{\lambda} |\alpha_{ab\lambda}|^2, \tag{4.A.2}$$

where $\mathcal{P}_x^{(X)}$ and $\mathcal{P}_y^{(Y)}$ are the projectors onto the eigenspaces of X and Y respectively. Then $\langle XY^\dagger\rangle = \sum_{x,y} xy^* P(x,y)$, $\langle X\rangle = \sum_x xP(x,y)$ etc. This allows for expressing $C(X,Y)$ as a non-linear functional of the probability distribution $P(x,y)$. Therefore, for the case of commuting Alice-Bob observables, $[A_i, B_j] = 0$ our bounds (4.2.2,4.2.3) can be considered restrictions on the possible joint probability distributions $P(a,b|i,j)$ in the quantum theory, defined exactly as in Eq. (4.A.2) modulo a replacement $X \to A_i$ and $Y \to B_j$.

For the case of non-commuting X and Y, one cannot define a joint eigenbasis, but rather eigenbases $|x\lambda\rangle$ of X and $|y\tilde{\lambda}\rangle$ of Y. One can still expand any state

$$|\psi\rangle = \sum_{x} \alpha_{x\lambda}|x\lambda\rangle \tag{4.A.3}$$

and define

$$\begin{aligned} W(x,y) &= \mathrm{Tr}|\psi\rangle\langle\psi|\mathcal{P}_x^{(X)}\mathcal{P}_y^{(Y)} \\ &= \sum_{x',\lambda,\lambda',\tilde{\lambda}} \alpha_{x'\lambda'}\alpha_{x\lambda}^*\langle x\lambda|y\tilde{\lambda}\rangle\langle y\tilde{\lambda}|x'\lambda'\rangle. \end{aligned} \tag{4.A.4}$$

Moreover, $\langle XY^\dagger\rangle = \sum_{x,y} xy^* W(x,y)$, $\langle X\rangle = \sum_x xW(x,y)$ etc., leading to exactly the same expression of $C(X,Y)$ in terms of $W(x,y)$ as previously

in terms of $P(x,y)$. However, $W(x,y)$ is not a probability distribution as the r.h.s. of Eq. (4.A.4) can acquire complex values. $W(x,y)$ is a quasiprobability distribution (somewhat similar to the Wigner function) in the case of non-commuting X and Y. Therefore, when $[A_i, B_j] \neq 0$ can be considered as restrictions on the possible joint quasiprobability distributions $W(a,b|i,j)$.

4.B Measuring parafermionic observables

A system combining parafermions with charging energy was introduced in Ref. [150]. In such a system there is a charging energy associated with the total system charge $Q_{\rm tot} = \sum_j Q_j + Q_0$, where $Q_0 = 2en_C$ is the charge of the proximitizing superconductor, and n_C is the number of Cooper pairs in it. However, no energy cost is associated with different distributions of a given total charge over different SC domains. Therefore, the ground state of such a system has degeneracy $d^{N_{\rm SC}-1}$, where the reduction by a factor of d corresponds to fixing the system's total charge. The properties of operators $\alpha_{s,j}\alpha^\dagger_{s,k}$ acting in this reduced subspace are identical to those in the original system of parafermions with unrestricted total charge.

Introducing charging energy allows for designing a relatively simple protocol for measuring $\alpha_{s,j}\alpha^\dagger_{s,k}$ (both parafermions have the same s!) [150]. A sketch of the measurement setup is shown in Fig. 4.1b. Two additional FQH edges (belonging to one of the puddles) are required in this setup. Tunneling of FQH quasiparticles is allowed directly between the two edges with tunnelling amplitude $\eta_{\rm ref}$ or between each edge and the corresponding parafermion $\alpha_{s,j/k}$ with amplitude $\eta_{j/k}$. As changing the charge of the parafermionic system is energetically costly, the leading non-trivial process resulting from coupling of the edges to the parafermions is co-tunneling of quasiparticles: a quasiparticle is transferred between the edges, while the parafermion state is changed via $\alpha_{s,j}\alpha^\dagger_{s,k}$ and the effective tunneling amplitude is $\eta_{\rm cot} \simeq -\eta_k\eta_j^*/E_C$, where E_C is the charging energy. The two processes, direct and parafermion-mediated tunneling of a quasiparticle between the edges, interfere quantum-mechanically. When a voltage bias V is applied between the edges, the tunneling current between the edges is sensitive to this interference:

$$I_{\rm T} \propto |V|^{2\nu-1}\,{\rm sgn}V \times \left(|\eta_{\rm ref}|^2 + |\eta_{\rm cot}|^2 + 2\kappa{\rm Re}\left[\eta^*_{\rm ref}\eta_{\rm cot}\alpha_{s,j}\alpha^\dagger_{s,k}\right]\right), \quad (4.B.1)$$

where κ is the interference suppression factor due to finite temperature

and other effects, $\mathrm{Re}\,[A] = \left(A + A^\dagger\right)/2$, and $|V|$ is assumed to be much larger than the temperature T of the probing edges. As a result, by measuring I_T, one can measure the operator $\mathrm{Re}\left[e^{i\varphi}\alpha_{s,j}\alpha_{s,k}^\dagger\right]$ with phase φ depending on the phases of η_ref and η_cot. Thus, one can measure the system in the eigenstates of $\alpha_{s,j}\alpha_{s,k}^\dagger$ employing the fact that the eigenvalues of the $\alpha_{s,j}\alpha_{s,k}^\dagger$ are discrete: for a generic φ, distinct eigenvalues of $\alpha_{s,j}\alpha_{s,k}^\dagger$ correspond to distinct eigenvalues of $\mathrm{Re}\left[e^{i\varphi}\alpha_{s,j}\alpha_{s,k}^\dagger\right]$. Alternatively, through tuning the phase φ, one can measure independently $\mathrm{Re}\left[\alpha_{s,j}\alpha_{s,k}^\dagger\right]$ and $\mathrm{Im}\left[\alpha_{s,j}\alpha_{s,k}^\dagger\right] = \mathrm{Re}\left[e^{-i\pi/2}\alpha_{s,j}\alpha_{s,k}^\dagger\right]$, and combine the measurement results for calculating the expectation value $\langle\alpha_{s,j}\alpha_{s,k}^\dagger\rangle$.

4.C How to measure correlations of non-commuting observables

4.C.1 Measuring correlations of non-commuting parafermionic observables

Here we discuss how one can measure the correlators $\langle A_j\,(B'_k)^\dagger\rangle$ for non-commuting parafermionic observables. The procedure outlined in Appendix 4.C.2 enables one to measure $\langle\{A_j,(B'_k)^\dagger\}\rangle$, where $\{X,Y\}$ denotes the anti-commutator of operators X and Y, using weak measurements [67, 68]. For the observables defined in Sec. 4.3.2, the following permutation relation holds: $A_j\,(B'_k)^\dagger = (B'_k)^\dagger\,A_j e^{-2i\pi\nu}$. Therefore, $\langle\{A_j,(B'_k)^\dagger\}\rangle = \langle A_j\,(B'_k)^\dagger\,(1+e^{2i\pi\nu})\rangle = 2\langle A_j\,(B'_k)^\dagger\rangle e^{i\pi\nu}\cos\pi\nu$, and measuring $\langle\{A_j,(B'_k)^\dagger\}\rangle$ is sufficient for measuring $\langle A_j\,(B'_k)^\dagger\rangle$.

The rest of this appendix is dedicated to designing weak measurements of the required type and adapting the protocol of Appendix 4.C.2 to measuring parafermionic observables. Note that this measurement method is specific to the particular implementation of parafermions. We start with the measurement protocol discussed in Appendix 4.B. Suppose one of the additional FQH edges involved in the protocol has voltage V applied to it, while the other edge is grounded. The current injected to the first edge is $I_\mathrm{in} = \nu e^2 V/h$, while the tunneling current between the edges is I_T, cf. Eq. (4.B.1). Suppose one measures the current for time t, so that the number of quasiparticles injected into the system is $N = I_\mathrm{in}t/(\nu e)$. The number of quasiparticles q tunneling within the time window will be fluctuating around the average $\langle q\rangle = pN = I_\mathrm{T}t/(\nu e)$ with $p = I_\mathrm{T}/I_\mathrm{in}$. The

expression for I_{T} in Eq. (4.B.1) is valid as long as $|I_{\mathrm{T}}| \ll |I_{\mathrm{in}}|$. In this regime, tunneling of different quasiparticles can be considered independent, and thus the probability of observing tunneling of q quasiparticles should be approximated well by the binomial distribution

$$P(q) = C_N^q p^q (1-p)^{N-q}, \quad C_N^q = \frac{N!}{q!(N-q)!}. \tag{4.C.1}$$

If one measures for a sufficiently long time, i.e., $N \gg 1$, the binomial distribution is well-approximated by the Gaussian distribution

$$P(q) \approx \frac{1}{\sqrt{2\pi N p(1-p)}} \exp\left(-\frac{(q-pN)^2}{2Np(1-p)}\right). \tag{4.C.2}$$

Depending on the eigenvalue $-e^{i\pi\nu(r+1/2)}$ of the measured observable $\alpha_{s,j}\alpha^{\dagger}_{s,k}$, the tunneling probability $p = p_0 + \delta p_r$, with

$$p_0 \propto |\eta_{\mathrm{ref}}|^2 + |\eta_{\mathrm{cot}}|^2, \tag{4.C.3}$$

$$\delta p_r \propto -2\kappa\, |\eta_{\mathrm{ref}}|\, |\eta_{\mathrm{cot}}| \cos\left(\pi\nu r + \pi\nu/2 + \varphi\right), \tag{4.C.4}$$

where $\varphi = \arg(\eta^*_{\mathrm{ref}}\eta_{\mathrm{cot}})$, cf. Eq. (4.B.1). From now on we assume $|\eta_{\mathrm{cot}}| \ll |\eta_{\mathrm{ref}}|$, $p_0 \ll 1$ and $p_0 N \gg 1$. Then the average number of tunneled quasiparticles is $\langle q\rangle_r = p_0 N + \delta p_r N$, while the size of fluctuations in the measured values of q is of the order σ:

$$\sigma = \sqrt{2Np(1-p)} = \sqrt{2Np_0}\left(1 + O(|\eta_{\mathrm{cot}}/\eta_{\mathrm{ref}}|, p_0)\right).$$

The parameter determining the distinguishability of different r, and thus the measurement strength, is $\delta p_r N/\sigma \propto \left|\frac{\eta_{\mathrm{cot}}}{\eta_{\mathrm{ref}}}\right| \sqrt{N}$. For sufficiently large $\left|\frac{\eta_{\mathrm{cot}}}{\eta_{\mathrm{ref}}}\right| \sqrt{N}$, the scheme thus implements a strong measurement, while the limit $\left|\frac{\eta_{\mathrm{cot}}}{\eta_{\mathrm{ref}}}\right| \sqrt{N} \ll 1$ implies a weak measurement.

Denoting the initial state of parafermions as $\sum_r \psi_r |r\rangle$ and using some approximations, one can derive the state of the system after switching on the tunnel couplings for time t,

$$|\tilde{\Phi}\rangle = \sum_{r,q,\lambda} f_\lambda(q,r)\psi_r \left(\frac{\eta_{\mathrm{ref}} - \eta_{\mathrm{cot}} e^{i\pi\nu(r+1/2)}}{\left|\eta_{\mathrm{ref}} - \eta_{\mathrm{cot}} e^{i\pi\nu(r+1/2)}\right|}\right)^q |r\rangle |q,\lambda\rangle, \tag{4.C.5}$$

where λ represents additional quantum numbers of the edges. It follows from Eq. (4.C.2) that:

$$\sum_\lambda f^*_\lambda(q,r) f_\lambda(q,r) = \mathcal{N}^2 \exp\left[-\frac{(q-\langle q\rangle_r)^2}{2Np_0}\right]\left[1 + O\left(\left|\frac{\eta_{\mathrm{cot}}}{\eta_{\mathrm{ref}}}\right|, p_0\right)\right]$$

, with normalization factor $\mathcal{N} = (2\pi N p_0)^{-1/4}$. Having not performed the calculation, we make a plausible assumption that also

$$\sum_\lambda f_\lambda^*(q,r) f_\lambda(q,r') = \mathcal{N}^2 \times \exp\left[-\left(q - \frac{\langle q\rangle_r + \langle q\rangle_{r'}}{2}\right)^2 \times \frac{1}{2Np_0} - \frac{(\langle q\rangle_r - \langle q\rangle_{r'})^2}{8Np_0}\right] \times \left[1 + O\left(\left|\frac{\eta_{\rm cot}}{\eta_{\rm ref}}\right|, p_0\right)\right]. \quad (4.C.6)$$

Further assuming the limit $\left|\frac{\eta_{\rm cot}}{\eta_{\rm ref}}\right| p_0 N \ll 1$, we can neglect $\eta_{\rm cot} e^{i\pi\nu(r+1/2)}$ in Eq. (4.C.5) and obtain that for our purposes one can replace $|\tilde{\Phi}\rangle$ with

$$|\Phi\rangle = \mathcal{N}\sum_{r,q} \psi_r \exp\left[-\frac{(q - \langle q\rangle_r)^2}{4Np_0}\right] \times \left[1 + O\left(\left|\frac{\eta_{\rm cot}}{\eta_{\rm ref}}\right| p_0 N, \left|\frac{\eta_{\rm cot}}{\eta_{\rm ref}}\right|, p_0\right)\right] |r\rangle|q\rangle, \quad (4.C.7)$$

which brings us to weak measurements of the type considered in Appendix 4.C.2.

Consider now two weak measurements accessing A_j and $(B'_k)^\dagger$ performed one after the other, with the number of quasiparticles tunneled in each of the measurements being q_1 and q_2. Repeating the calculation of Appendix 4.C.2, we obtain

$$\langle (q_1 - p_0 N)(q_2 - p_0 N)\rangle \propto \langle \mathrm{Re}\left[e^{i\varphi} A_j\right] \mathrm{Re}\left[e^{i\varphi'} (B'_k)^\dagger\right]\rangle \times \left[1 + O\left(\left|\frac{\eta_{\rm cot}}{\eta_{\rm ref}}\right| p_0 N, \left|\frac{\eta_{\rm cot}}{\eta_{\rm ref}}\right|, p_0\right)\right]. \quad (4.C.8)$$

Using Eq. (4.C.16), one sees that by choosing different phases φ, φ', one can measure $\langle\{A_j, (B'_k)^\dagger\}\rangle = 2\langle A_j (B'_k)^\dagger\rangle e^{i\pi\nu}\cos\pi\nu$.

4.C.2 Measuring correlations of non-commuting observables with weak measurements

Here we discuss how to measure the averages $\langle\{A, B\}\rangle$ of non-Hermitian non-commuting A and B, where $\{A, B\} = AB + BA$, with the help of weak measurements. Our protocol uses essentially the same measurement

procedure as in Refs. [153–155], and is similar in spirit (yet has important differences) to Refs. [156, 157]. We note in passing that by more elaborate methods, one can measure also the expectation value of a commutator [145]. However, measuring the anti-commutator will suffice for our purposes. We first discuss how to measure correlations of Hermitian non-commuting observables, and then generalize the scheme to non-Hermitian observables.

Suppose one wants to measure the average $\langle\{A,B\}\rangle = \langle\psi|\{A,B\}|\psi\rangle$, where A and B are *Hermitian* non-commuting operators, and $|\psi\rangle$ is some quantum state. Introduce the eigenbases of A and B: $A|a\rangle = a|a\rangle$, $B|b\rangle = b|b\rangle$. Any system state $|\psi\rangle$ can then be written as $|\psi\rangle = \sum_a \psi_a|a\rangle = \sum_{a,b}\psi_a|b\rangle\langle b|a\rangle$ with some coefficients ψ_a. We assumed that there is no degeneracy in the spectra of A and B; generalization of the below consideration for the case with degeneracy is straightforward.

Consider two detectors, D_1 and D_2 each having coordinate Q_j and momentum P_j operators, $[P_j, Q_k] = -i\delta_{jk}$, with j and k having values 1 and 2. Prepare the system and detectors in initial state

$$|\Phi_{in}\rangle = |\psi\rangle|D_{1,in}\rangle|D_{2,in}\rangle, \tag{4.C.9}$$

$$|D_{j,in}\rangle = \mathcal{N}\int dq_j \exp\left(-\frac{q_j^2}{2\sigma^2}\right)|q_j\rangle, \tag{4.C.10}$$

where $|q_j\rangle$ is an eigenstate of Q_j with eigenvalue q_j, and $\mathcal{N} = \left(\pi\sigma^2\right)^{-1/4}$.

The Hamiltonian describing the system and the detectors is

$$H(t) = \lambda_1(t)H_1 + \lambda_2(t)H_2, \tag{4.C.11}$$

$$H_1 = P_1 A, \quad H_2 = P_2 B, \tag{4.C.12}$$

where the coupling constants $\lambda_j(t) = 0$ except for $\lambda_1(t) = g/T$ for $t \in (0;T)$ and $\lambda_2(t) = g/T$ for $t \in (T;2T)$. Then after the system has interacted with the detectors, their state is

$$\begin{aligned}|\Phi\rangle = e^{-igH_2}e^{-igH_1}|\Phi_{in}\rangle \\ = \mathcal{N}^2\sum_{a,b}\int dq_1 dq_2 \psi_a\langle b|a\rangle|b\rangle|q_1\rangle|q_2\rangle \\ \times\exp\left(-\frac{(q_1-ga)^2}{2\sigma^2} - \frac{(q_2-gb)^2}{2\sigma^2}\right).\end{aligned} \tag{4.C.13}$$

Measuring Q_1 and Q_2 of the detectors and calculating their correlations then yields the desired quantity. Indeed,

$$\begin{aligned}\langle\Phi|Q_1Q_2|\Phi\rangle &= \mathcal{N}^4 \sum_{a,a',b} \psi_a^*\psi_{a'}\langle a|b\rangle\langle b|a'\rangle \\ &\quad\times \int dq_2 q_2 \exp\left(-\frac{(q_2-gb)^2}{\sigma^2}\right) \\ &\quad\times \int dq_1 q_1 \exp\left(-\frac{(q_1-g(a+a')/2)^2}{\sigma^2} - \frac{g^2(a-a')^2}{4\sigma^2}\right) \\ &= \sum_{a,a',b} \alpha_a^*\alpha_{a'}\langle a|b\rangle\langle b|a'\rangle \frac{g^2}{2} b(a+a') \exp\left(-\frac{g^2(a-a')^2}{4\sigma^2}\right). \quad (4.C.14)\end{aligned}$$

Provided that $g\,|a-a'| \ll 2\sigma$ for all a, a' (which is the condition for weakness of the measurement), one obtains

$$\begin{aligned}&\langle\Phi|Q_1Q_2|\Phi\rangle \\ &\qquad= \frac{g^2}{2}\sum_{a,a',b} \psi_a^*\langle a|\,(a|b\rangle b\langle b| + |b\rangle b\langle b|a')\,\psi_{a'}|a'\rangle \\ &\qquad= \frac{g^2}{2}\langle\psi|\{A,B\}|\psi\rangle. \quad (4.C.15)\end{aligned}$$

Suppose now one wants to measure $\langle\{A,B\}\rangle = \langle\psi|\{A,B\}|\psi\rangle$ for *non-Hermitian* A and B. Define the real and imaginary part of each operator: $R_A = (A+A^\dagger)$, $I_A = i(A^\dagger - A)/2$, and similarly for B. It is easy to see that $\{A,B\} = \{R_A,R_B\} - \{I_A,I_B\} + i\{I_A,R_B\} + i\{R_A,I_B\}$. Then

$$\begin{aligned}\langle\{A,B\}\rangle = \langle\{R_A,R_B\}\rangle - \langle\{I_A,I_B\}\rangle \\ + i\langle\{I_A,R_B\}\rangle + i\langle\{R_A,I_B\}\rangle. \quad (4.C.16)\end{aligned}$$

Each of the averages in the r.h.s. can be measured using the protocol for Hermitian observables outlined above. Then combining them according to Eq. (4.C.16) yields the desired correlation of non-Hermitian non-commuting observables.

4.D Extra numerical data on the bounds for correlations in the system of parafermions

In the main text, Table 4.1, we provided the results of testing the bounds on correlations for two sets of observables, non-signaling (A_0, A_1, B_0, B_1) and signaling (A_0, A_1, B'_0, B'_1). Here, in Table 4.2, we present the results for several more sets of observables. Namely, we checked what happens when the roles of Alice's operators A_0 and A_1 are exchanged, and similarly for Bob. Apart from that, we also tested the sets involving $B_2 = B_0^\dagger B_1 = \alpha_{L,5}\alpha_{L,6}^\dagger$ and $B'_2 = B_0'^\dagger B'_1 = \alpha_{R,6}\alpha_{R,5}^\dagger$; $[B_2, A_j] = [B'_2, A_j] = 0$, with A_j, B_j, B'_j defined in Eqs. (4.3.11–4.3.16). In all the sets we tested, all Alice's and Bob's operators commute when Bob uses unprimed observables; some of Alice's operators do not commute with some of the Bob's observables when Bob uses primed observables, B'_j.

Note that all the sets we have tested obey all bounds except for relation (4.2.5). The latter is obeyed by all the non-signaling sets (when Bob uses B_j observables) and violated by all the signaling sets (when Bob uses B'_j observables). This strengthens the numerical evidence that relation (4.2.5) is a good candidate for quantifying the effect of signaling on quantum correlations.

In principle, the system of parafermions has many more possible sets of observables. First, assigning different parafermions to Alice and Bob, one can have different local algebras at Alice's and Bob's sites, as well as different Alice-Bob commutation relations. We investigate them in part by switching the order of A_0 and A_1 etc. or replacing B_1 with B_2 in Table 4.2. While this does not exhaust all the possibilities, the numerical results we do have, indicate that our conclusions are likely to hold in the cases we did not check. An even richer set of algebras can be accessed by using operators beyond quadratic in parafermions, e.g., $\left(\alpha_{s,j}\alpha_{s,k}^\dagger\right)^n$ or $\alpha_{s,j}^2\alpha_{s,k}^\dagger\alpha_{s,l}^\dagger$, as well as arbitrary linear combinations of quadratic operators, e.g., $x\alpha_{s,j}\alpha_{s,k}^\dagger + y\alpha_{s,j}\alpha_{s,l}^\dagger$. While investigating our bounds with these would be an interesting non-trivial check, we believe that the more important task is understanding and proving the role of Theorem 4 and bound (4.2.5) in the general context.

Bound:			I_3	**Tsirelson type**	**TLM-type, l.h.s/r.h.s.**	**L.h.s. of (4.2.4)**	**L.h.s. of (4.2.5)**
Theoretical maximum			2.91 [152]	$2\sqrt{2}$ ($\approx$ 2.83)	1	1	**1 (if assumptions hold)**
Parafermion maximum	**Alice's operators**	**Bob's operators**					
	A_0, A_1	B_0, B_1	2.60	2.44	0.71	0.74	1.00
	A_0, A_1	B'_0, B'_1	2.60	2.82	1.00	1.00	1.56
	A_1, A_0	B_1, B_0	2.60	2.44	0.71	0.74	1.00
	A_1, A_0	B'_1, B'_0	2.60	2.82	1.00	1.00	1.56
	A_0, A_1	B_1, B_0	2.60	2.22	0.71	0.62	1.00
	A_0, A_1	B'_1, B'_0	2.60	2.71	1.00	0.97	1.56
	A_0, A_1	B_0, B_2	2.60	2.44	0.71	0.74	1.00
	A_0, A_1	B'_0, B'_2	2.00	2.23	1.00	0.75	1.50
	A_0, A_1	B_2, B_0	2.60	2.22	0.71	0.62	1.00
	A_0, A_1	B'_2, B'_0	2.00	2.44	1.00	0.75	1.50

Table 4.2: Characterization of bounds on non-local correlations for various sets of parafermionic observables. Similarly to the Table 4.1, the maximal values achieved with parafermionic observables ('Parafermion maximum') are compared to the theoretical maximum.